

## 1.5.5 Heusler alloys

### 1.5.5.1 Introduction

This chapter reviews the physical properties of Heusler and related compounds. It contains new information which has primarily appeared since the last review was undertaken in 1985 [88W1]. Thus it is still necessary to access the first review for older information and for detailed analysis of topics such as atomic order in Heusler alloys. The same format has been used in this review as before, with each subsection focusing on a particular property with the results collated according to composition and constituent elements. For those subsections dealing with new topics e.g. Magneto-optics, background information is provided to facilitate the interpretation of the results, otherwise reference must be made to the first review [88W1]. S.I. units have been used throughout with the recommendation of Crangle and Gibbs [94C1] for magnetic units adopted.

### 1.5.5.2 Structural properties

#### 1.5.5.2.1 Crystallography

Heusler alloys are defined as ternary intermetallic compounds at the stoichiometric composition  $X_2YZ$  which have the  $L2_1$  structure (Fig. 1). The unit cell (Fig. 1) comprises four inter-penetrating fcc sublattices with origins at (000),  $(\frac{1}{4}\frac{1}{4}\frac{1}{4})$ ,  $(\frac{1}{2}\frac{1}{2}\frac{1}{2})$  and  $(\frac{3}{4}\frac{3}{4}\frac{3}{4})$ . Permitted Bragg reflections occur when the Miller indices are unmixed which gives rise to three types of structure factor.

(i)  $h, k, l$  all odd

$$F(111) = 4 \left| (f_A - f_C)^2 + (f_B - f_D)^2 \right|^{\frac{1}{2}}$$

(ii)  $h, k, l$  all even and  $h + k + l = 4n + 2$

$$F(200) = 4 |f_A - f_B + f_C - f_D| \quad (1)$$

(iii)  $h, k, l$  all even and  $h + k + l = 4n$

$$F(220) = 4 |f_A + f_B + f_C + f_D|$$

where  $f_A, f_B, f_C$  and  $f_D$  are the average scattering factors for the atoms in the respective sublattices. For Heusler alloys with the  $L2_1$  structure and site occupation as shown in Fig. 1 the structure amplitudes become

$$(i) \quad F(111) = 4 |f_Z - f_Y|$$

$$(ii) \quad F(200) = 4 |f_Z + f_Y - 2f_X| \quad (2)$$

$$(iii) \quad F(220) = 4 |f_Z + f_Y + 2f_X|$$

Possible types of atomic disorder and models describing disorder were extensively discussed in the first review [88W1]. Although there is an infinite number of ways in which the atoms XYZ can be distributed over the lattices ABCD there are several types of preferential disorder which frequently occur. These are shown in Fig. 2.

An alternative representation of the preferential types of atomic order which can occur is shown in Fig. 3 [88W1]. In this representation, the occupation of the atoms XYZ over the sites ABCD can only take the discrete values 1, 0.5 or 0.3 (0.66).

For a compound with the  $L2_1$  structure, the most frequent type of preferential disorder to occur as a function of temperature is B2. In this process the Y and Z atoms interchange sites with total B2 order being achieved when half the Y and Z atoms have interchanged sites. The consequence of this type of ordering process is that the intensity of the (111) superlattice reflection is reduced to zero. The  $\text{Pd}_2\text{MnIn}$  system is particularly susceptible to this type of disorder. The critical temperatures of the order disorder transitions  $L2_1 \leftarrow T_2 \rightarrow B2 \leftarrow T_1 \rightarrow A2$  in several Heusler compounds have been determined. (A2 represents complete disorder (Table 1) where the atoms XYZ are randomly distributed over the 4 sites ABCD (Figs. 4 and 5)). Unfortunately the prototype Heusler alloy  $\text{Cu}_2\text{MnAl}$  has a complicated phase diagram [88W1] making it difficult to stabilise a single  $L2_1$  structure at room temperature.

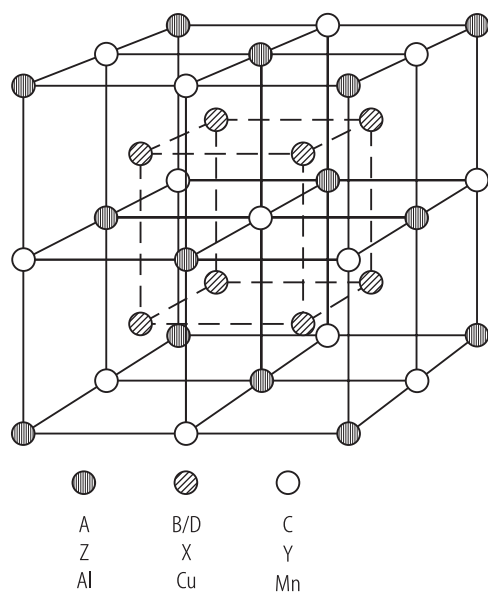


**Fig. 1.** Heusler  $L2_1$  structure with unit cell of space group  $Fm\bar{3}m$  ( $O_h^h$ ) described in terms of 4 interpenetrating fcc sublattices A, B, C, D. A and C sites have point symmetry  $m\bar{3}m$  (octahedral site) and the B and D sites  $4\bar{3}m$  (tetrahedral site).

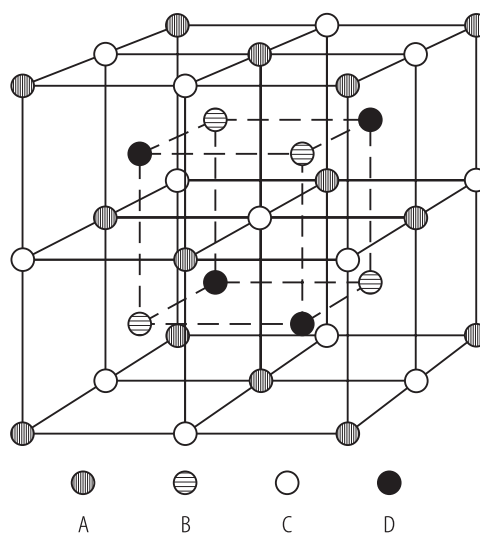


**Fig. 2.** Seven principal possible ordered structures formed from four interpenetrating fcc sublattices A, B, C, D. Principal ordered structures: A2: all lattices identically filled; B2: A filled as C, B filled as D; B32: A filled as B, C filled as D;  $L2_1$ : B filled as D;  $D0_3$ : B, C and D identically filled; C1: A filled as C, D void;  $C1_b$ : D void.

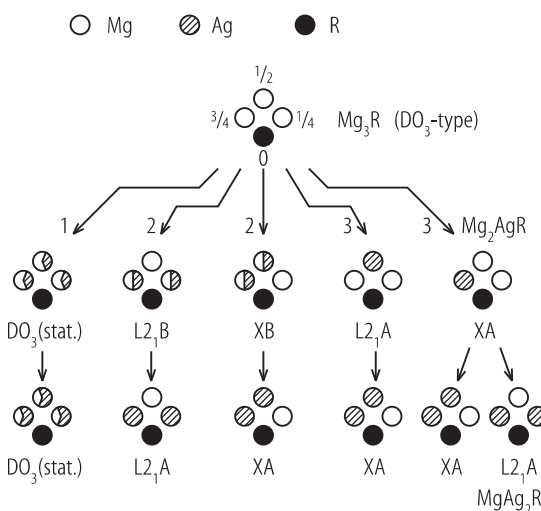


**Fig. 3.** Growth pattern for  $\text{Mg}_3\text{R} \rightarrow \text{Mg}_2\text{AgR} \rightarrow \text{MgAg}_2\text{R}$  [88B1]. stat: statistical distribution.

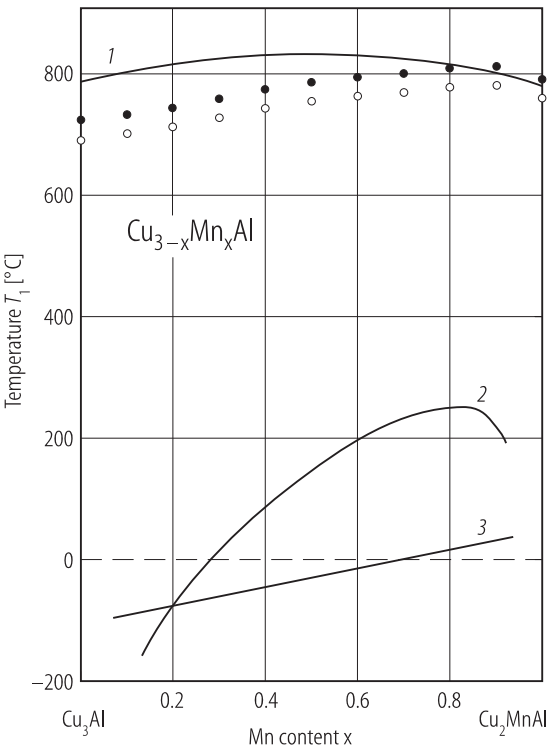


**Fig. 4.**  $\text{Cu}_{3-x}\text{Mn}_x\text{Al}$ . Phase diagram. The full line 1 represents the values of B2 - A2 ordering temperature  $T_1$  calculated with the assumption of the lack of structural vacancies whereas the lines 2 and 3 assume their existence [83S2].

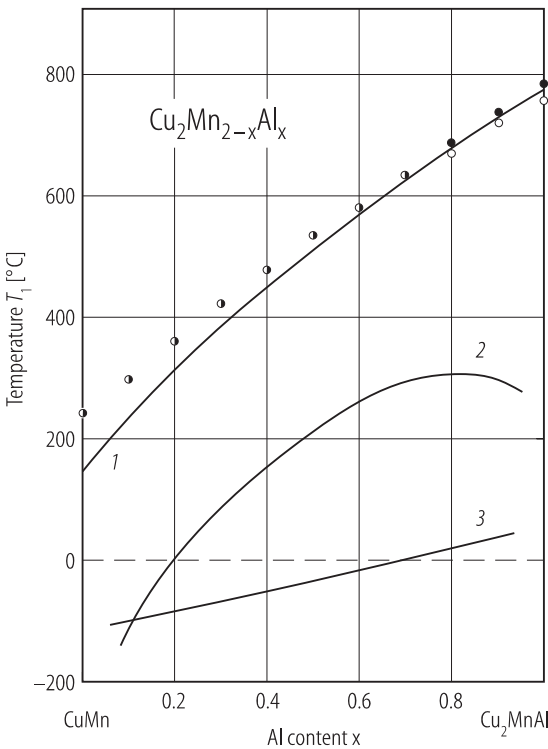


**Fig. 5.**  $\text{Cu}_2\text{Mn}_{2-x}\text{Al}_x$ . Phase diagram. The full line 1 represents the values of B2 - A2 ordering temperature  $T_1$  calculated with the assumption of the lack of structural vacancies whereas the lines 2 and 3 assume their existence [83S2].

**Table 1.** A summary of the ordering temperatures  $T_1$  (B2-A2) and  $T_2$  ( $\text{L}_{21}$ -B2) for several Al-based Heusler alloys. The calculated value  $T_1$  was obtained from the configurational free energy of the system [83S2].

Alloy	Experimental results				Calculated
	$T_2$ [°C]		$T_1$ [°C]		$T_1$ [°C]
	heating	cooling	heating	cooling	
$\text{Cu}_2\text{MnAl}$	883	903	1063	1063	1074
$\text{Ni}_2\text{MnAl}$	993	993	1223	1223	1268
$\text{Co}_2\text{MnAl}$	993	1013	1250	1240	1310
$\text{Pd}_2\text{MnAl}$	980	980	1280	1280	1332
$\text{Pt}_2\text{MnAl}$	1040	1040	1300	1300	1371

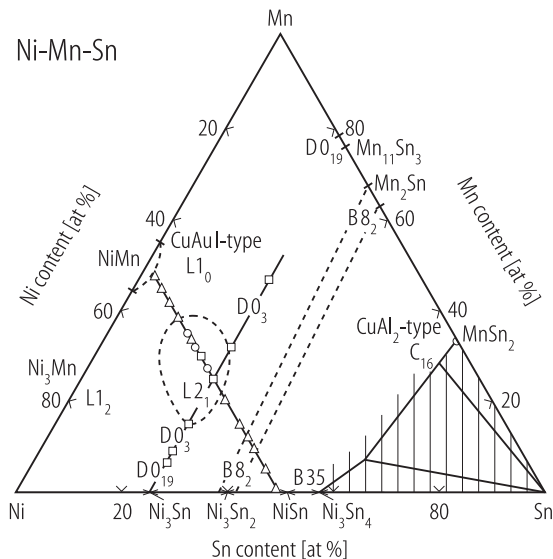
**Table 2.** Cu<sub>2</sub>MnAl. A summary of the phase content after various heat treatments [83K2].  $T_a$ : annealing temperature for 24 hours.

$T_a$ [°C]	Volume fractions of phases [%]				Properties of $\beta$ phase	
	$\gamma$	T	$\beta$ Mn	$\beta$	$a$ [Å]	$T_C$ [°C]
150				100	5.962	327
200				100	5.959	326
250				100	5.963	326
300				100	5.962	327
350	5	12		84	5.961	339
400	44	25	17	7	5.960	317
450	24		25	51	5.896	57
500	15		33	52	5.913	113
550	6		35	59	5.919	139
600			18	82	5.921	202
650			18	82	5.930	239
700				100	5.961	326

### 1.5.5.2.2 Ternary phase diagrams

There are very few ternary phase diagrams reported for Heusler alloys. Those which have appeared since 1985 [88W1] have been primarily associated with the investigation of the mechanical properties.

#### Ni–Mn–Sn

**Fig. 7.** Ni–Mn–Sn. Ternary phase diagram [83W1].